Volume [illegible] Number [illegible] [illegible]

NIGERIAN JOURNAL OF PHYSICS

ISSN [illegible] website: [illegible]

NIGERIAN JOURNAL OF PHYSICS

NIP

Published By

THE NIGERIAN INSTITUTE OF PHYSICS

Supported by Education Trust Fund

Interpretation of High Resolution Aeromagnetic Data for Basement Depth estimates in Northwestern Nigeria: A preliminary Assessment for Energy Prospectivity

Shehu A. T.[1], Nwankwo L. I.[2] and Salako K. A.[3]

[1] Physics Unit, Centre for Preliminary and Extra-Mural Studies, Federal University of Technology Minna, Niger State, Nigeria.
[2] Department of Physics, University of Ilorin, Kwara State, Nigeria.
[3] Department of Physics, Federal University of Technology Minna, Niger State. Nigeria.

E-mail address: atshehu2006@gmail.com , linwankwo@unilorin.edu.ng, kasalako2012@gmail.com

Abstract:

Energy source diversification and sustainability is no longer a slogan but a necessity in Nigeria, this, work on geophysical exploration for oil and gas in Northern part is in line with the target for diversifying energy exploitation beyond Niger Delta region for economic reason. The Total Magnetic Intensity (TMI) data covering the study area of longitudes 3.50 ºE and 7.00 ºE and latitudes 10.00 ºN and 14.00 ºN was divided into thirty seven blocks of 55 km by 55 km for the purpose of two-dimensional Fourier analysis in order to estimates depth to the basement in the area. Results from spectral analysis indicated two magnetic source depths, which account for deeper and shallower magnetic sources. Linear segment from the low frequency portion of the spectral plot is due to deeper source effects, representing the depth to the top of magnetic source (H2) interpreted as sedimentary thickness varies between 0. 47 km and 3.05 km. The sedimentary thickness increases from the south to north, temperatures at depth for each section were also estimated in line with Fourier's law of heat conduction in the crust. These results agree with earlier geophysical work done in the area, which revealed that the area is not potentially viable for fossil fuel energy.

Key words: Aeromagnetic, spectral depth, Sedimentary, Anomaly and Sokoto Basin

Introduction

In modern geophysical surveys, aeromagnetic anomaly data reflect the lateral variation in the earth's magnetic field. These variations are related to changes of structure, susceptibility of magnetic materials in the crust, temperature increases with depth, and related minerals present in the rock. Airborne survey can be utilized as a multipurpose data in different fields such as exploration, medical physics and environmental studies (Manzella, 1999).
The advantages of airborne survey include rapidity, cost effectiveness, large extent of surveyed area and the possibility of application in inaccessible region where no other geophysical methods can be utilized (Chinwuko *et al.,* 2012). Aeromagnetic surveys flown in Nigeria in the 1970's with a flight line spacing of 2 km, average terrain clearance of 152.4 m, and a nominal tie line spacing of 2 km have played a key role in understanding the country's regional geology. However due to their low resolution, they have become of limited use. As a result, a nationwide High Resolution Airborne Geophysical (Magnetic, electromagnetic and Radiometric) surveys were carried out for the Nigerian Geological Survey Agency in 2009. The acquisition, processing and compilation of the new data, which was partly financed by the Federal Government of Nigeria and the World Bank as part of major project known as the Sustainable Management for Mineral Resources Project, were carried out by Fugro Airborne Surveys Ltd. The High Resolution Airborne Geophysical Digital Data were acquired from aircrafts flown at height of 80 m with 500 m line spacing, 80 m mean terrain clearance and the tie line spacing of 500 m. This new low height survey data which is digitally high in resolution has been adjudged to be better than the previous 1970's low resolution analogue data by the NGSA.

Geology and Location of the Study Area

The Sokoto Basin located in the northwestern part of Nigeria is bounded by latitudes 10.00 °N and 14.00 °N and longitudes 3.50 °E and 7.00 °E (Figure 1). It has total surface area of approximately 111, 925 km^2, which cuts across six states in Nigeria namely: Kaduna, Katsina, Kebbi, Niger, Sokoto and Zamfara., is one of the inland basins in Nigeria. It is a sedimentary basin and consists of gentle undulating plain, underlain by basement rocks consisting of igneous and metamorphic rocks.

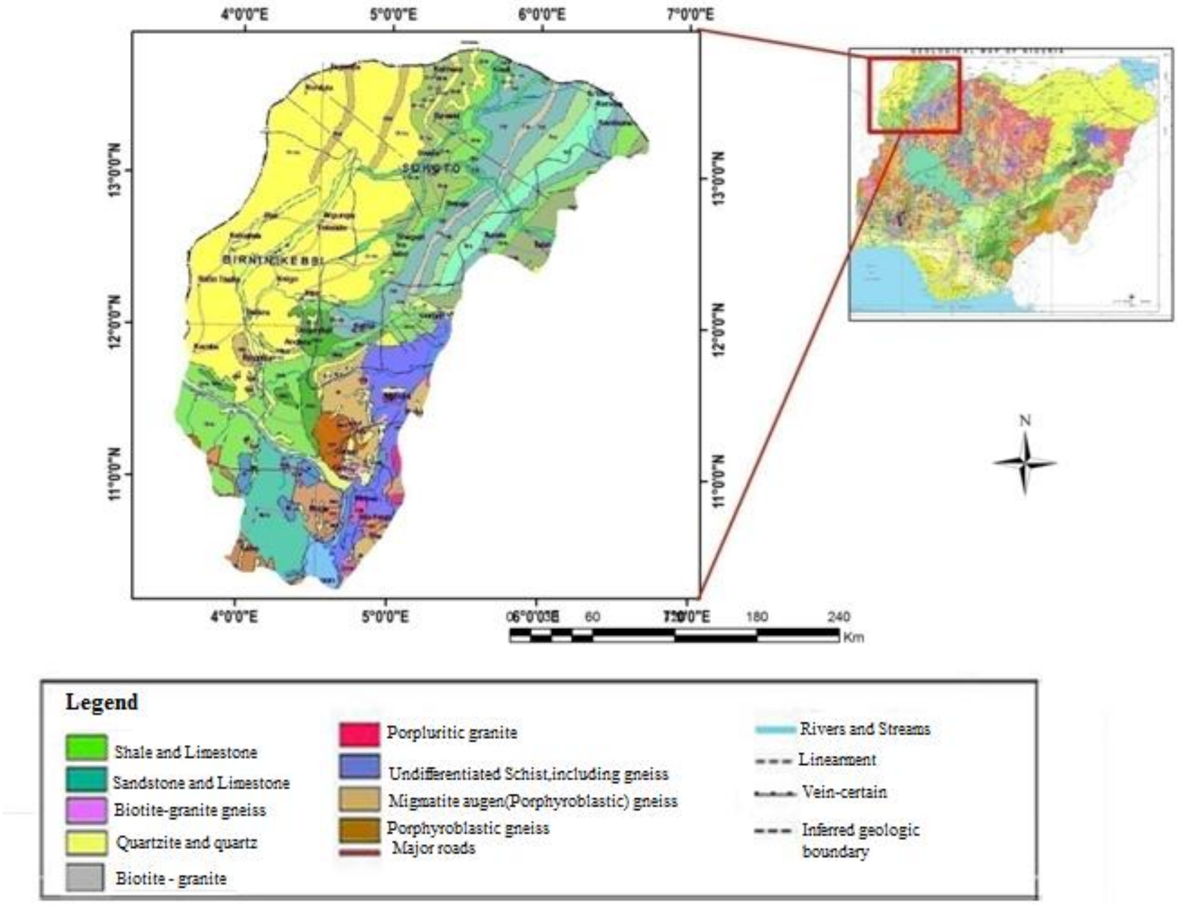

Figure 1: Geologic map of Sokoto Basin (Adapted from Nigerian Geological Survey Agency, 2006).

The Sahel climate or tropical dry climate which is the predominant climate type in the area is dominated by two opposing air masses, tropical maritime and tropical continental. The tropical maritime is moist and blows from the Atlantic ocean while the tropical continental air, which is dry blows from the Sahara Desert. The basin is a semi-arid region marked by two distinct conditions: wet and dry season's weather. The annual rainfall is between 500 mm in the north and 1300 mm to the south. Within the Sokoto basin there is considerable variation in rainfall distribution with mean annual rainfall ranging from 350 mm at kurdula in the extreme northwest and 670 mm at Sokoto Airport. The rainy season, which usually lasts from June to September of each year, or early October depending on the rain fall pattern for each year while the dry season which is dry and hot with temperatures exceeding 39 °C. February, March and April are the hottest months, where daytime temperatures can exceed 45 °C (Balogun, 2003). Dry harmattan season is between November and March. Moreover, the basin is characterized by two extreme temperatures relative to tropical position.

In the Sokoto basin water resource can be divided into precipitation, surface water and ground water.
Sokoto basin is a region with great potential for future large-scale economic development, due to warm and bountiful mineral resources, geothermal energy, farmland and water through irrigation project and borehole thereby boosting food production. The most important economics mineral in the Sokoto basin are the industrial minerals consisting of clays, limestone, gypsum and phosphate other are ironstone and laterites, gravel and lignite.

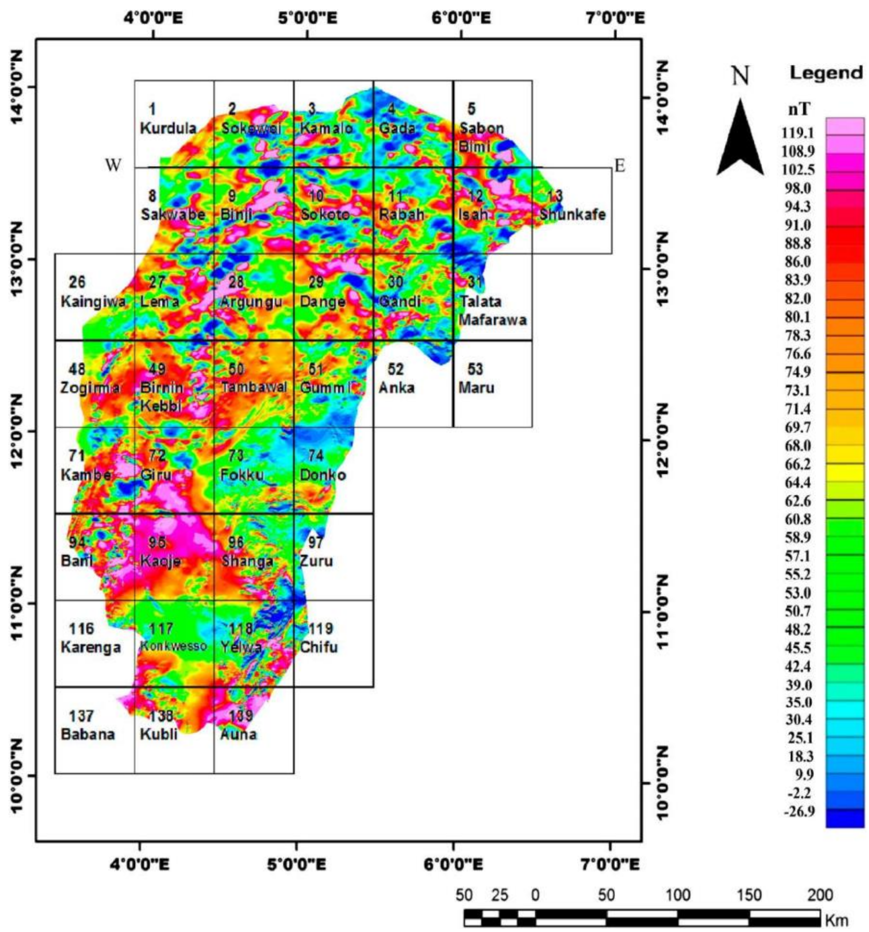

Figure 2: **Total magnetic intensity map (TMI) of entire Sokoto basin with superimposed federal survey half degree sheets and showing major towns flown over. A constant 33,000 nT removed.**

Materials and Methodology

Materials

Thirty eight (38) digital half degree HRAM maps (sheet number 1-5, 8-13, 26-31, 48-53, 71-74, 94-97, 116-119 and 138-139) on a scale of 1:100,000 with a total 7,426,917 data points were used in this study. The whole data, which were procured from the Nigerian Geological Survey Agency (NGSA) and assembled into composite total magnetic field intensity (TMI) map (Figure. 2), range between 32,487.96 and 33,423.06 nT with an average of 33,060.70 nT and a standard deviation of 38.314. Regional correction which was based on the International Geomagnetic Reference Field (IGRF) was made as well as subtraction of a constant TMI value of 33,000 nT by the NGSA before the eventual publication as HRAM Maps. No further processing was made for the reason that Ravat *et al.* (2007), after comparing different spectral methods of estimating depth to the magnetic sources from high resolution magnetic anomaly data, strongly recommended that filtering to remove arbitrary regional fields should be avoided.

Methodology

Magnetic method for estimating the sedimentary thickness of sedimentary fill on the basement, was based on the theory of Bhattacharyya and Leu (1975) which examine the shape of isolated magnetic anomalies when the anomalies data are processed by Fourier analysis of aeromagnetic to get the power spectrum of magnetic anomalies

The Magnetic sheets were join together to form composite TMI data (Figure 2) which was divided into thirty eight (38) sections for the purpose of 2D spectral Fourier analysis while ensuring that essential parts of the anomaly were not cut out by the sections. Each block covers a square area of 55 km x 55 km. However, sheet number 53 (Maru) with insufficient data was omitted. Hench, section was Fast Fourier Transformed (FFT) and radial average energy spectrum obtained. This produced column for logs of energy and the corresponding frequencies, energy spectrum plots were plotted for each of the thirty seven sections, Figure 3 shows energy Spectra of selected Sections. Linear segment from the low frequency portion of the spectral, representing contributions from the deep-seated magnetic sources could be estimated from the slope of each energy spectral plot and subsequently used to estimate H2 while slope of the linear segment from the high frequency portion of each plots were used to estimate depth H1 (Table 1). The H2 is the thickness of the sedimentary fill on top of the basement, this estimates could also be used for locating major structures in basement rocks.

3.3: Theory of Spectral Analysis

Spectral Fourier analysis was applied out on the high resolution aeromagnetic data. The Fourier Transform is represented mathematically as shown below:

$$f(\mathrm{t}) = \mathrm{a}_o + \sum_{n=1}^{\infty} (\mathrm{a}_n \mathrm{cosnt} + \mathrm{b}_n \mathrm{sinnt}) \quad (1)$$

$$a_o = \frac{1}{2}\int_{-\pi}^{\pi} f(\mathrm{t})\,\mathrm{dt} \quad (2)$$

$$a_n = \frac{1}{\pi}\int_{-\pi}^{\pi} f(\mathrm{t})\,\mathrm{cosntdt} \quad (3)$$

$$b_n = \frac{1}{\pi}\int_{-\pi}^{\pi} f(\mathrm{t})\,\mathrm{sinntdt} \quad (4)$$

where a_o, a_n and b_n are Fourier coefficients and their estimations is referred to as Fourier analysis. $n = 0, 1, 2, 3, \ldots$

This geophysical analysis is commonly applied on regularly spaced data such as aeromagnetic data using Discrete Fourier Transforms (Spector and Grant, 1970; Hahn, 1976; Murthy and Mishra, 1980):

$$f(\mathrm{n}) = \mathrm{F(n)}\,\mathrm{e}^{j\phi(\mathrm{n})} \frac{1}{N} \sum_{u=1}^{N} f(\mathrm{u})\,\mathrm{e}^{-t(\frac{2m\pi n}{N})\mathrm{u}} \quad (5)$$

where the given time series are $f(1), \mathrm{f}(2), \ldots, \mathrm{f(N)}$ for N data points, at equal spacing.

In magnetic analysis, it is useful to have proposed models, such as sphere, cylinders, fault, etc. which cause the anomaly at the surface. For this reason, the total magnetic field anomaly ΔT, measured in the direction of geomagnetic field is given by (Spector and Grant, 1970; Hahn, 1976; Murthy and Mishra, 1980):

$$T = \frac{1}{2} A[\ln \frac{(x - t\cot d)^2 + (\mathrm{h+t})^2}{x^2 + h^2} + B[\tan^{-1}\{\frac{(x - t\cot d)}{(h+t)}\} - \tan^{-1}(\frac{x}{h})] \quad (6)$$

where $A = 2kH_o(1 - \cos^2 i \cos^2 h\lambda)\sin d \cos(d - 2\beta)$ and $B = 2kH_o(1 - \cos^2 i \cos^2 h\lambda)\sin d \sin(\mathrm{d} - 2\beta)$, I = magnetic inclination, d = dip of the step, t = thickness of the step, k = susceptibility constant, H_o= geomagnetic field and the angle I and h are combined into a single variable defined by tan β = $\tan i / \sin \lambda$.

The Fourier transform and modified transform of equation (8) is given respectively as:

$$\Delta T(\omega) = \frac{\pi}{\omega} e^{-h\omega}[(A - A\cos(t\omega\cot d)e^{-t\omega} - B\sin(t\omega\cot d)e^{-t\omega} - j\cos(t\omega\cot d)e^{-t\omega} - A\sin(t\omega\cot d)e^{-t\omega} - B] \quad (7)$$

$$\Delta T(\omega) = \pi\,\mathrm{e}^{-h\omega}[A - A\cos(t\omega\cot d)e^{-t\omega} - B\sin(\mathrm{t}\,\omega\mathrm{cotd})\,\mathrm{e}^{-t\omega} + j\cos(t\omega\cot d)e^{-t\omega} - A\sin(\mathrm{t}\,\omega\mathrm{cotd})\,\mathrm{e}^{-t\omega} - B] \quad (8)$$

The modified Amplitude Spectrum is consequently given by

$$A(\omega) = \mathrm{Ce}^{-h\omega}(1 + e^{-2t\omega} - 2\cos(\mathrm{t}\,\omega\mathrm{cotd})\,\mathrm{e}^{-t\omega})\frac{1}{2} \quad (9)$$

where $C = 2\pi KH_o(1 - \cos^2 i \cos^2 \lambda)\sin d$

Taking the logarithm of equation (9):

$$\ln A(\omega) = \ln\mathrm{C} - m\omega + \frac{1}{2}\ln[1 + e^{-2t\omega} - 2\cos(\mathrm{t}\,\omega\mathrm{cotd})\,\mathrm{e}^{-t\omega}] \quad (10)$$

For sufficiently larger value of ω, equation (10) reduces to:

$$\ln A(\omega) = \ln\mathrm{C} - m\omega \quad (11)$$

where $\ln A(\omega)$ is energy spectrum and ω is frequency (cycle/km).

The depth h to the causative bodies can subsequently be calculated using the relation (Spector and Grant, 1970):

$$h = -\frac{m}{4\pi} \quad (12)$$

In this work, the graph of $\ln A(\omega)$ against frequency (ω) was plotted and the gradient (m_1) for the deeper source and gradient (m_2) for shallow source were deduced. The depths h_1 and h_2 are therefore given by the respective slopes of straight line segments of low and high frequency portions of energy spectrum (Spector and Grant, 1970; Hahn, 1976; Murthy and Mishra, 1980):

$$h_1 = \frac{m_1}{4\pi} \quad \text{and} \quad h_2 = \frac{m_2}{4\pi} \quad (13)$$

Estimation of Temperature at Depth

Temperature at depth expresses the fossile energy potential of the crust, in exploration geophysics temperature range at depth in which oil forms is referred to as oil window, commonly found in sedimentary formation with thickness up to or above 3.0 km, in the range of 60 - 120 °C (Chinwuko *et al.,* 2012). Below the minimum temperature the organic matter remain trapped in the form of kerogen and above the maximum temperature the oil is converted to natural gas through the process of thermal cracking. The geothermal heat flow in the crust is governed by Fourier's law. The temperatures at depth for each section were estimated using the approach of (Chinwuko *et al.,* 2012).

$$T_h = mH_2 + T_\theta \quad (14)$$

where,

T_h = temperature at depth,

m = geothermal gradient

H_2 = Sedimentary thickness,

T_θ = maximum Land Surface Temperature

The average geothermal gradient in Sokoto basin was given by (Nwankwo and Shehu 2015) as 33.99 °C/km and average maximum Land Surface Temperature for the region is 39 ^{0}C (Shehu and Nwankwo, 2015).

Results and Discussion

The exponential rate of decay of magnetic power signal is expressed in the graph of log of spectral energy against frequency; energy spectral plots for the thirty seven sections were plotted. This forms the bases for evaluation of H_1 and H_2, plots for section 1 and 2 are shown in Figure 3,

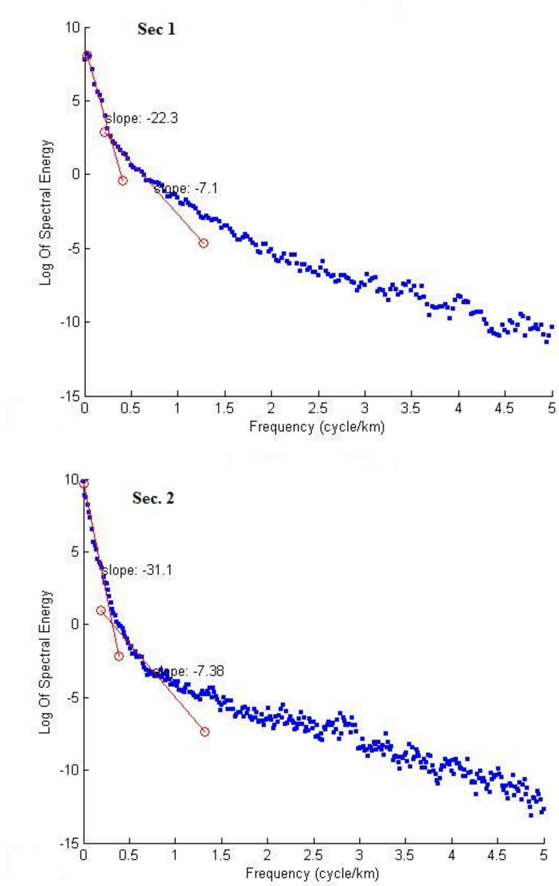

Figure 3: Energy Spectra of selected Sections

Table 1 gives estimates of depth to magnetic sources and temperature at depth**.** The table shows that the deeper magnetic sources vary from vary from 0.47 to 3.05 km with an average of 1.93 km, while the shallow sources vary from 0.13 to 1.08 km with an average of 0.47 km. These results agree with previous depth to shallow magnetic sources of 0.22 – 0.96 km with an approximate average value of 0.46 km obtained by (Adetona *et al.*, 2007). The sedimentary thicknesses which represent depth to deeper magnetic sources agree with the estimated 1.00 – 3.00 km (Obaje *et al.*, 2013) and 1.23 – 3.10 km (Bonde *et al.*, 2014). The result also agree with documented data Figure (2) from NGSA Abuja-Nigeria, low magnetic anomalies areas corresponds to sections with high sedimentary thickness due to basement top depression while high magnetic anomalies area corresponds to sections with low sedimentary thickness as evidenced in sections 23 and 24. The sedimentary thickness increases from the south to the north Table 1, shows the estimated depths to the magnetic sources and temperature at depth corresponding to each values of H2, temperature at depths for most section is found to be higher than the threshold temperature of 115 °C for the concealment of oil formation from organic matter in sediment if all other conditions for oil and gas accumulation are favorable (Wright *et al.,* 1985). Similarly areas with sedimentary thickness value of 3.00 km or above indicate potential (Obaje *et al.*, 2014) if other conditions are favorable. Statistically the sedimentary fill on the basement in the study area is immature for oil but mature for gas. This area is highly prospective for gas due to high temperature geothermal energy in the area. Section 13 (Lema) with highest sedimentary fill on the basement with corresponding high depth temperature is the most probable area in the basin for oil and gas exploitation. Figure (4) is the Contour Map of estimated second magnetic layer (H2) depth Contour Interval of 0.10 km of the study area, portion filled in yellow represent areas with fairly high sedimentary thickness found in the northern part of the study area while area filled in black color represent areas with low sedimentary thickness found in the southern part of the study area. Figure 5 is the Basement topographic map of the second layer layer (H2) depth shows that the sedimentary fill on top of the basement in the northern part is thicker than the southern part ,interpreted to corresponds to many troughs, trenches, ditches, sinks, pits and holes (indicated in Brown). While the southern part (indicated in Blue) corresponds to basement high (ridge) with low sedimentary fill on the basement. The maps (Figure 4 -5) are trending NE-SW in the northern part and NW-SE trending in the southern part. The observed trends are similar to the regional trending faults in the basin which are prominent at Dange and Gilbedi, where the palaeocene beds have been truncated by several WSW-ENE faults (Wright, 1976, Kogbe, 1979).

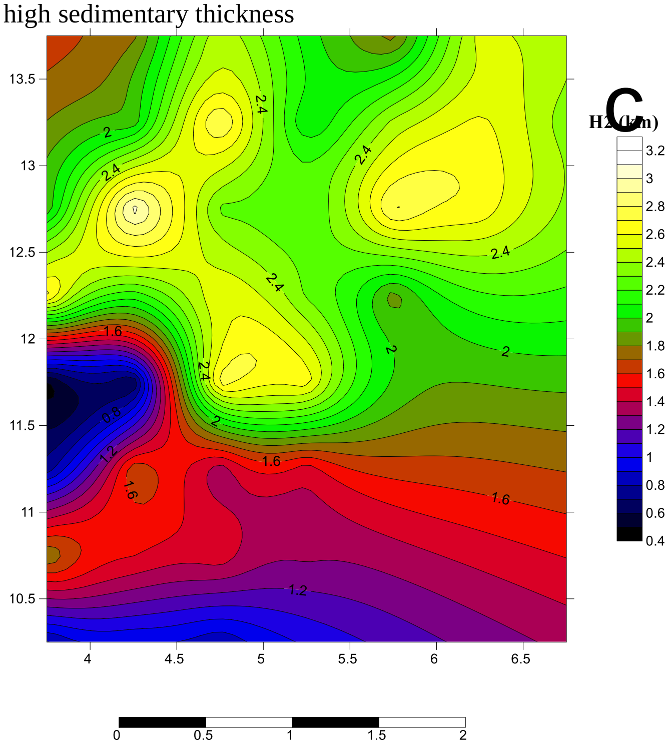

Figure 4: Contour Map of estimated second magnetic layer (H2) depth Contour Interval of 0.10 km of the study area.

Table 1: Estimates of depth to magnetic sources

Sections	Longitude (ºE)	Latitude (ºN)	H_1 (Km)	H_2 (Km)	Depth temp (ºC)
1	4.0 - 4.5	14.0-13.5	0.57	1.77	99.15
2	4.5- 5.0	14.0-13.5	0.59	2.47	122.89
3	5.0 - 5.5	14.0-13.5	0.39	2.05	108.59
4	5.5- 6.0	14.0-13.5	0.32	1.76	98.61
5	6.0 - 6.5	14.0-13.5	0.28	2.54	125.04
6	4.0 - 4.5	13.5-13.0	0.27	1.94	104.81
7	4.5- 5.0	13.5-13.0	0.55	2.82	134.76
8	5.0 - 5.5	13.5-13.0	0.13	2.01	106.97
9	5.5- 6.0	13.5-13.0	0.72	2.43	121.27
10	6.0 - 6.5	13.5-13.0	0.84	2.62	127.74
11	6.5 - 7.0	13.5-13.0	0.31	2.34	118.30
12	3.5 - 4.0	13.0-12.5	0.32	1.93	104.55
13	4.0 - 4.5	13.0-12.5	1.08	3.05	142.31
14	4.5- 5.0	13.0-12.5	0.76	2.28	116.14
15	5.0 - 5.5	13.0-12.5	0.30	2.20	113.45
16	5.5- 6.0	13.0-12.5	0.43	2.82	134.76
17	6.0 - 6.5	13.0-12.5	0.47	2.67	129.36
18	3.5 - 4.0	12.5-12.0	0.41	2.74	131.79
19	4.0 - 4.5	12.5-12.0	0.36	2.14	111.56
20	4.5- 5.0	12.5-12.0	0.45	2.58	126.39
21	5.0 - 5.5	12.5-12.0	0.35	2.28	116.41
22	5.5- 6.0	12.5-12.0	0.35	1.85	101.85
23	3.5 - 4.0	12.0-11.5	0.22	0.47	55.08
24	4.0 - 4.5	12.0-11.5	0.37	0.59	59.07
25	4.5- 5.0	12.0-11.5	0.89	2.75	132.33
26	5.0 - 5.5	12.0-11.5	0.55	2.65	128.82
27	3.5 - 4.0	11.5-11.0	0.33	0.74	64.09
28	4.0 - 4.5	11.5-11.0	0.57	1.68	95.91
29	4.5- 5.0	11.5-11.0	0.56	1.34	84.32
30	5.0 - 5.5	11.5-11.0	0.68	1.44	87.82
31	3.5 - 4.0	11.0-10.5	0.28	1.80	99.96
32	4.0 - 4.5	11.0-10.5	0.34	1.50	89.98
33	4.5- 5.0	11.0-10.5	0.41	1.46	88.63
34	5.0 - 5.5	11.0-10.5	0.49	1.32	83.78
35	3.5 - 4.0	10.5-10.0	0.51	0.79	65.70
36	4.0 - 4.5	10.5-10.0	0.39	0.91	69.75
37	4.5- 5.0	10.5-10.0	0.56	0.82	66.78
Average			**0.47**	**1.93**	

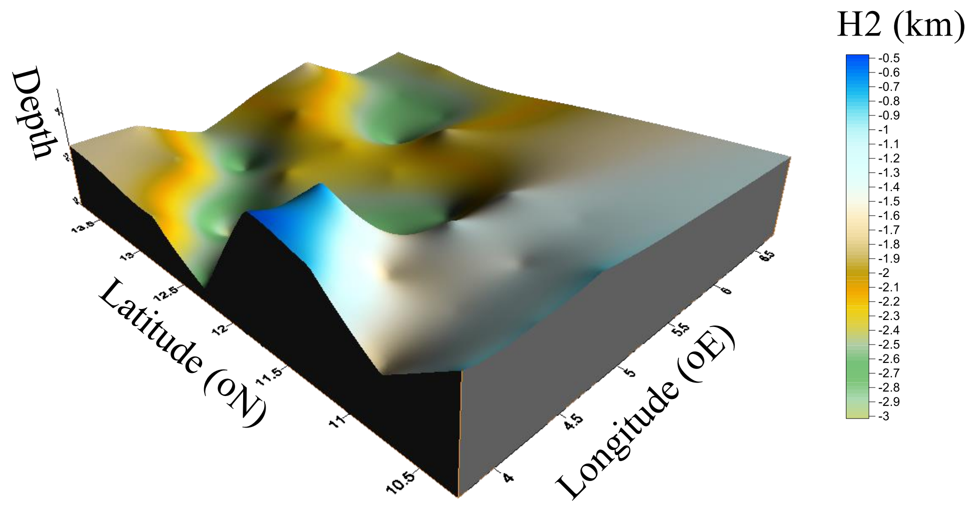

Figure 5: Basement topographic map of the second layer layer (H2) depth

Conclusion

A preliminary Assessment for energy prospectivity

The result of the spectral analysis of the high resolution regional aeromagnetic data over the entire Sokoto basin suggested the existence of two clear layers of magnetic source. The deeper sources vary between 0.47 km - 3.05 km with an average of 1.93 km, these deeper sources effect represented by the low frequency component of the energy spectrum are considered to be the thickness of the sedimentary formation. The shallow layer depth varies from 0.13 km – 1.08 km with an average of 0.47 km, these shallow sources effect represented by the high frequency component of the energy spectrum represents the near surface contribution. The temperature at depth is reasonably high with the highest depth temperature of 143 ^oC in section 13.

It has been shown in previous works that minimum sedimentary thickness of 3.00 km with a threshold depth temperature of 115 ^oC is required for oil accumulation provided all other conditions are favorable for oil formation. Base on this, prospect area for fossil fuel energy (oil and/or gas) is section 13 (Lemu) which correspond to a sink. The observed prospect area constitute just 2.7 % of the analyzed area. High temperature at depth indicates high geothermal gradient which enhances early formation of oil. Consequently it can be concluded that the study area is immature for oil but mature for gas owing to high temperature at depth observed in 15 sections representing 41% of the analyzed area. This work on preliminary Assessment for energy prospectivity revealed that energy options exist in Sokoto basin that could be explored for sustainable economy in Nigeria. The observed prospect area is recommended for detail future seismic and geothermal investigation such as drilling for bottom hole temperature (BHT).

Acknowledgment

The authors are grateful to the Nigerian Geological Survey Agency, for granting a financial rebate on the purchase of the HRAM data, and the Federal University of Technology. Minna- Nigeria. For granting the major author a research leave to undertake the study.

References

Adetona, A. A., Udensi E. E. and Agelaga G. A. (2007). Determination of depth to buried rocks under the lower Sokoto Basin, Nigeria using aeromagnetic data. *Nigerian Journal of Physics*, 19: 275-283.

Aku, M. O., Umego, M. N., and Musa, A.O. (2013), Gravity study of rocks in the Schist belts of Northwest Nigeria. *Nigerian Journal of Physics*. Vol. 24: 83 – 90.

Bhattacharyya, B.K., Leu, L.K., (1975). Spectral analysis of gravity and magnetic anomalies due to two dimensional structures. *Geophysics* Vol. 40 pp. 993 - 1013.

Bonde, D. S., Udensi, E.E., Momoh, M., Joshua, B.W and Abbas, M. (2014). Basement Depth Estimates of Sokoto Sedimentary Basin, Northwestern Nigeria, Using Spectral Depth Analysis. *SGJ of Geology and Exploration Research*. Vol. 1 (4), pp.78-85.

Bott, M. H. P. (1973). Inverse methods in the interpretation of magnetic and gravity anomalies in methods in computational physics (*B, Alder, S., Fernbach and B. A. Bolt, Eds.)*, 13: 133 – 162.

Chinwuko, A. I., Onwuemesi, E. K., Onuba, L.O. and Nwokeabia, N. C.(2012). Interpretation of Aeromagnetic Anomalies over parts of Upper Benue Trough and Southern Chad Basin, Nigeria. *Advance in Applied Science Research Journal;* Vol. 3(3), pp 1757 -1766.

Federal Ministry of Mines and Steel Development, Nigerian Geological Survey Agency (2010), Airborne *Geophysical Digital Data Dissemination Guidelines*. pp. 1 – 23

Finn, C. A., Ravat, D., (2004). Magnetic depth estimates and their potential for constraining crustal composition and heat flow in Antarctica. *EOS. Trans. AGU 85 (47) (Fall meeting Suppl.,* Abstract (1179-1236).

Grant, N. K., (1978). Structural distinction between a metasedimentary cover and underlying basement in 600 m. y. *Old pan –African domain of northwest Nigeria, West African Geol. So. Am. Bulletin.* Vol. (89), pp. 50-58.

Hahn, A. E., kind, G. and Mishra, D. C. (1976). Depth estimation of magnetic source by means of Fourier Amplitude Spectra. *Geophysical Prospecting* vol. (24), pp. 287.

Kasidi, S. and Nur, A. (2013a). Spectral Analysis of Magnetic Data over Jalingo and Environs Northeastern Nigeria. *International Journal of Science and Research*,Vol.2 (2) pp. 447-454.

Kearey, P. and Brooks, M. (2000). An introduction to geophysical exploration. *Blackwell Science*. Vol. 2(5) 112 – 237.

Kogbe, C. A. (1979). Geology of the Southeastern (Sokoto) sector of the lullemmeden Basin. *Bulletin. Department of Geology, Ahmadu Bello University* 2(1). pp. 91 -237.

Kogbe, C.A., (1981). Cretaceous and Tertiary of the Iullemmeden Basin of Nigeria (West Africa).*Cretaceous Research* 2,129-186.

Kurowska, E., Schoeneich, K., (2010). Geothermal exploration in Nigeria. *Proceedings World Geothermal Congress. Bali, Indonesia,* pp. 25-29 (April.).

Nwankwo, L. I., (2015). Estimation of depths to the bottom of magnetic sources and ensuing geothermal parameters from aeromagnetic data of Upper Sokoto Basin, Nigeria. *Elsevier Journal on Geothermics* 54, 76-81

Nwankwo, L. I. and Shehu, A. T. (2015). Evaluation of Curie-point depths, geothermal gradients and near-surface heat flow from high-resolution aeromagnetic (HRAM) data of the entire Sokoto Basin, Nigeria. *Journal of Volcanology and Geothermal Research. 305, 45-55*. Publisher: Elsevier.

Obaje, N.G., (2009). Geology and Mineral Resources of Nigeria. *Springer Publishers*, Germany
. Vol.43(2), pp.1 – 203.

Obaje, N. G., Aduku, M. and Yusuf I. (2013). The Sokoto Basin of Northwestern Nigeria: A Preliminary Assessment of the Hydrocarbon prospectivity. *Petroleum Technology Development Journal*, Vol.3(2).pp. 66 – 80.

Ravat, D., Pignatelli, A., Nicolosi, I. And Chiappini, M. (2007). A study of spectral methods of estimating the depth to the bottom of magnetic sources from near-surface magnetic anomaly data. *Geophysical Journal International* vol.169(2) pp. 421 – 434.

Shehu, A. T. and Nwankwo, L. I. (2015). Application of spaceborne high-Resolution Thermal Infrared in the detection of geothermal probable areas in the Sokoto Basin Nigeria. *Nigeria Journal of Engineering and Applied Sciences*. Publisher: Federal University of Technology Minna, Nigeria.Vol 3(2) pp 123= 132

Spector, A. and Grant, F. S. (1970). Statistical models for interpreting aeromagnetic data *Geophysics* vol. 35, pp. 293 – 302.

Wright, J. B., Hastings, D., Jones, W. B. and Williams, H. R., (1985). Geology and Mineral
Resources of West Africa. *George Allen and Urwin*, London. 90 – 120.